Materials Reports: Solidwaste and Ecomaterials

Journal Homepage: www.sciopen.com/journal/3078-4093

Original Research Report

Sustainable recycling of phosphogypsum and recycled concrete aggregate into base course for pavement: Mix design and durability evaluation

Jinxiong Huang [1, 2, 3], Xiong Xu [1, 2, 3, *], Kazi Rajibul Alam [4], Yang Wu [1], Chiyao Qu [1], Jiapei Wang [1]

[1] School of Civil Engineering and Architecture, Wuhan Institute of Technology, Wuhan 430073, China

[2] State Key Laboratory of Green and Efficient Development of Phosphorus Resources, Wuhan Institute of Technology, Wuhan 430205, China

[3] Hubei Provincial Engineering Research Center for Green Civil Engineering Materials and Structures, Wuhan Institute of Technology, Wuhan 430073, China

[4] School of International Education, Wuhan Institute of Technology, Wuhan 430073, China

Abstract: Phosphogypsum (PG) and recycled concrete aggregates (RCA) are commonly used in base course materials as substitutes for natural aggregates. However, the use of PG and RCA alone may lead to issues such as poor water stability and insufficient durability. Therefore, this study considered using sodium metasilicate nonahydrate (SMN), calcium stearate emulsion (CSE), and emulsified styrene-butadiene rubber (ESBR) as additives for preparing base course materials to improve their water stability and durability. Dry-wet cycling test, freeze-thaw cycling test, dry shrinkage experiment, and fatigue test were conducted to evaluate the effects of the adopted additives on the comprehensive performance of a calcined PG (CPG)/RCA base course material. The results indicate that with the addition of SMN and CSE, the 28-day strength of CPG/RCA-SC increases to 8.29 MPa. After five freeze–thaw cycles, the residual compressive strength ratio of CPG/RCA-SC reaches 72%, which is substantially higher than that observed for the PG/RCA (36.7%) and for the CPG/RCA (50.6%). Furthermore, the incorporation of SMN, CSE, and ESBR reduces the 180-day drying shrinkage strain from 1172.5×10^{-6} for the RCA to 570×10^{-6} for the CPG/RCA-SCE. In terms of fatigue performance, the k-value is markedly increased from 1.083 for PG/RCA to 418.287 for CPG/RCA-SCE. Overall, the adopted additives can help largely consume PG and RCA into the base course for more sustainable and durable pavement applications.

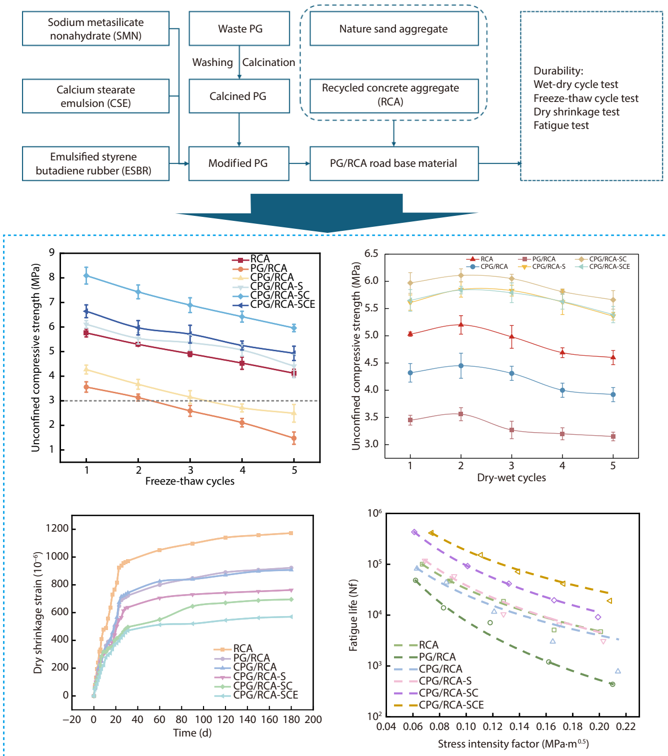

Keywords: base course, phosphogypsum, recycled concrete aggregates, water stability, durability

Citation: J. Huang, X. Xu, K. R. Alam, Y. Wu, C. Qu, J. Wang. Sustainable recycling of phosphogypsum and recycled concrete aggregate into base course for pavement: Mix design and durability evaluation. *Materials Reports: Solidwaste and Ecomaterials*, 2026, 2: 9520023. https://doi.org/10.26599/MRSE.2026.9520023.

*Correspondence to X. Xu, xxucea@wit.edu.cn

Received 12 November 2025; Received in revised form 31 December 2025; Accepted 18 January 2026

Tsinghua University Press | SciOpen

1. Introduction

The recycling and reuse of multiple solid wastes has been a common strategy in China towards sustainable and low-carbon developments, including industrial solid wastes like phosphogypsum (PG), municipal wastes like plastics and concrete, and other types[1-3]. PG is the by-product generated from the production of phosphoric acid by the wet method[4], which is primarily composed of 70%–90% dihydrate calcium sulfate ($CaSO_4{\cdot}2H_2O$), and contains small amounts of organic materials, radioactive substances, heavy metals, fluorine, and phosphorus[5,6]. It is reported that approximately 3–5 tons of PG are produced per ton of phosphoric acid produced[7,8]. In China, around 75–78 million tons of PG are produced annually, while the consumption rate is still very low, below 50%, leading to significant resource and environmental issues[9]. Therefore, it is very pressing to find a proper solution to largely recycle and reuse PG.

Currently, PG has been widely applied in the construction, agricultural, and chemical industries. Among these applications, road base construction, owing to its large consumption capacity, rapid material transformation, and relatively controllable safety risks, is regarded as one of the most promising pathways for the resource utilization of PG[10-12]. Because original PG is extremely sensitive to water, it is generally calcined at temperatures ranging from 100 °C to 200 °C for several hours prior to use, thereby inducing a crystal phase transformation from $CaSO_4 \cdot 2H_2O$ to calcium sulfate hemihydrate ($CaSO_4 \cdot 0.5H_2O$), with a conversion rate of approximately 70%–90%[13]. This calcination process enhances the specific surface area, activity, and reactivity of PG while reducing its sensitivity to moisture-induced damage[14]. For example, Liu et al.[15] reported that during the calcination of PG, soluble phosphorus impurities can be transformed into water-insoluble compounds such as CaP_2O_7. Deng et al.[16] demonstrated that composite cementitious materials produced by combining cement, fly ash, rice husk ash, and modified additives with calcined PG (CPG) exhibit enhanced mechanical properties and water resistance. Overall, CPG shows considerable potential for application in pavement base materials.

Except for PG, large amounts of concrete waste have been and continue to be produced from construction and demolition every day in cities like Wuhan in China due to large-scale renovations over the past few decades, and this trend is expected to continue in the future[17,18]. Recycled concrete aggregate (RCA) is a granular material made from leftover concrete. Concrete waste typically comes from construction projects, road maintenance, or demolition work[19,20]. Old concrete is recycled through processes like crushing, screening, washing, and other methods. These steps break it down into particles that meet the requirements for reuse in the construction of new concrete[17,21]. By reducing resource consumption in the construction industry, RCA helps decrease reliance on natural resources. Additionally, the recycling and reusing of concrete waste can reduce its negative impact on the environment by preventing large amounts of building waste from being burned or dumped in landfills[22,23]. Furthermore, using RCA can help save construction costs and contribute to a reduction in building carbon emissions, as it minimizes the need for new materials and reduces energy consumption in production[24]. However, the mere incorporation of these recycled materials into cement-stabilized base layers is often insufficient to overcome intrinsic performance limitations, necessitating the synergistic application of composite modifiers.

Recent studies have shown that compound chemical additives can effectively enhance the performance of this stabilizing layer. For instance, incorporating sodium metasilicate nonahydrate (SMN) into the pavement base material is conducive to the formation of calcium silicate hydrate gel, thereby enhancing the compressive strength of the mixture[25,26]. Similarly, calcium stearate emulsion (CSE) and emulsified styrene-butadiene rubber (ESBR) are also frequently used as modified components to enhance the long-term performance of materials. Wu et al.[27] found that introducing CSE into concrete could significantly enhance its water resistance. The 48-hour water absorption rate of the modified cement mortar with a CSE content of 0.8 wt% decreased by 39.02%, and its strength did not decline significantly. Yao et al.[28] discovered that ESBR can enhance the crack resistance and water stability of materials, thereby improving their durability. Therefore, it is necessary to develop a comprehensive approach (integrating effective modifiers like SMN, CSE, and ESBR) to address the technical limitations of RCA and PG in road base applications and to ensure the improvement of long-term durability of the pavement.

To address the insufficient durability of PG/RCA base course materials and the limited consideration of multi-additive synergistic effects in existing studies, this research investigates a composite modification strategy incorporating SMN as a strength-enhancing additive, CSE as a water-repellent additive, and ESBR as a flexibility-enhancing modifier. A systematic experimental program, including dry-wet cycling (WDCT), freeze-thaw cycling (FTCT), dry shrinkage (DST), and fatigue tests (FT), is conducted to comprehensively evaluate the durability performance of the modified PG/RCA base course materials. The results are expected to provide a more robust technical basis for the practical application of PG and RCA in pavement base engineering.

2. Research program

Based on a previous study[29], the optimal mixing dosages of SMN, CSE, and ESBR were determined as 2.2%, 0.32%, and 1.0% of the total mass, respectively. While the previous work mainly focused on mechanical properties, the present study extends the investigation to the durability performance. Fig. 1 shows the research flowchart of this study.

3. Materials and methods

3.1. Raw materials

3.1.1. Phosphogypsum

The phosphogypsum (PG) powders adopted in this study were supplied from a factory in Hubei province. Their original state is generally moist and agglomerated, with a dark-gray appearance. To better satisfy the application require-

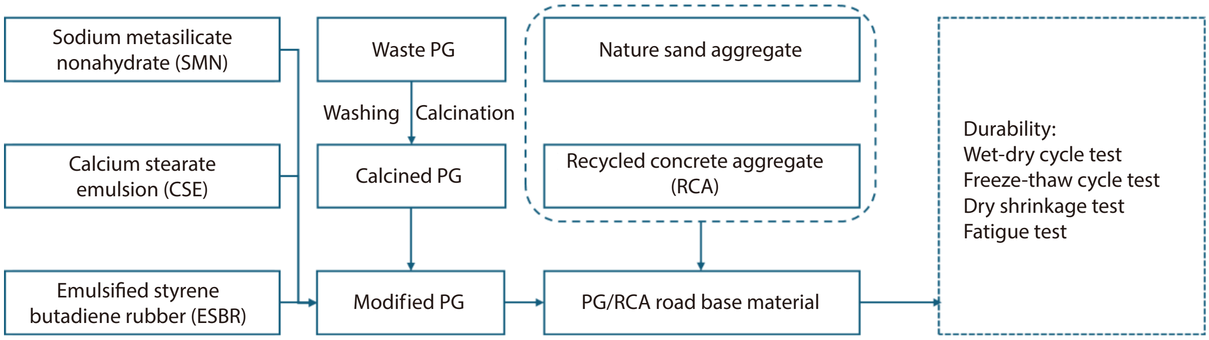

Fig. 1. Flowchart of this research plan.

ments, these original PG powders were calcined at approximately 160 °C for 2 h to remove part of the crystalline water for conversions towards hemi-hydrous gypsum ($CaSO_4 \cdot 0.5H_2O$). Calcination at 160 °C can decompose part of the fluorine- and phosphorus-bearing phases, reducing soluble impurities and heavy metal activity[30]. These calcined powders are denoted as CPG. Fig. 2 shows the surface appearances of PG and CPG. It is observed that the CPG powders have a smaller particle size and a much drier state in comparison with the original PG powders. In addition, the relative weight proportions of CaO and SO_3 in the original and calcined powders are approximately 30.72% and 40.20%, respectively, of the total chemical composition.

3.1.2. Aggregates

The aggregates used in this study include coarse recycled concrete aggregate (RCA) and fine natural aggregate (NA), as shown in Fig. 3. The coarse RCA, ranging in size from 4.75 mm to 19 mm, was sourced from a local factory in Wuhan city, while the fine NA, with a particle size of below 4.75 mm, was also provided by a local supplier. The measured values of their key physical properties are presented in Table 1.

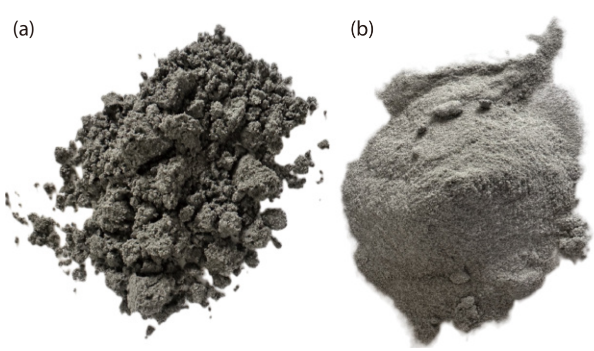

Fig. 2. Surface appearances of (a) PG and (b) CPG.

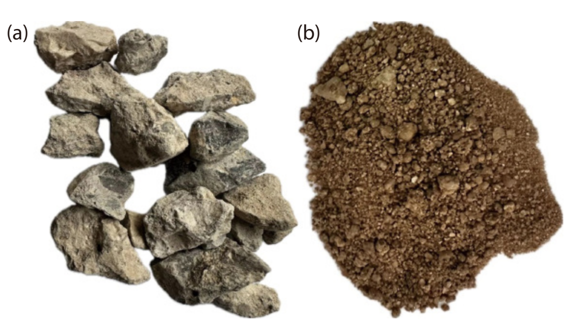

Fig. 3. Surface appearances of (a) RCA and (b) NA.

Table 1. Measured results of the main physical properties of the used aggregates.

Test item	Measured result	
	RCA	NA
Bulk density (kg m^{-3})	1190	1240
Apparent density (kg m^{-3})	2560	2597
Porosity (%)	0.47	-
Water absorption (%)	6.1	-
Crushing value (%)	15.9	-
Fineness modulus	-	2.94

Note: "-" indicates not measured or not applicable.

3.1.3. Cementitious materials

Using sodium metasilicate nonahydrate (SMN) as a strength-enhancing additive, calcium stearate emulsion (CSE) as a water-repellent additive, and emulsified styrene-butadiene rubber (ESBR) as a flexibility-improving additive, we aim to solve the durability issue. The cementitious materials used in this study include ordinary Portland cement, sodium metasilicate nonahydrate (SMN), and emulsified styrene-butadiene rubber (ESBR), all of which were purchased from the market. The cement used was ordinary Portland cement with a grade of P.O. 42.5, serving as the inorganic binder to stabilize the aggregates and CPG powders. SMN was incorporated as a strength-enhancing additive to create an alkaline environment that promotes hydration and cementation. ESBR was used as an organic flexibility-improving additive to physically bind the aggregates and CPG powders while also enhancing the water-resistant properties of the mixtures. The molecular structures and technical performance indicators of these materials are shown in Fig. 4 and Table 2.

3.1.4. Calcium stearate emulsion

Calcium stearate emulsion (CSE) is a white chemical liquid with the molecular formula of $C_{36}H_{70}CaO_4$, commonly used as a water-repellent additive in construction materials. In this study, it was utilized to mitigate the potential risk of moisture-induced damage caused by CPG powders and RCA aggregates[31]. The CSE was purchased from a supplier in Guangzhou City, China. The molecular structure and physical properties of CSE are presented in Fig. 5 and Table 3.

3.2. Preparation method

3.2.1. Mix design

(1) Aggregate gradation

This study substituted 20% by weight of the total aggre-

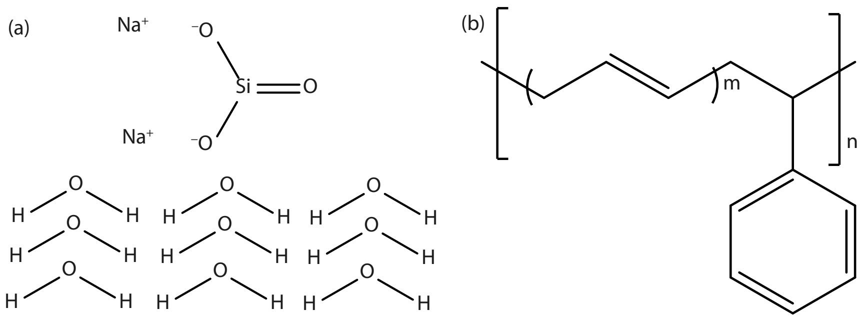

Fig. 4. The molecular structures of (a) SMN and (b) ESBR.

Table 2. Cement, SMN, and ESBR performance indicators.

Test item	Test result		
	P.O 42.5	SMN	ESBR
Stability	Qualified	-	-
Initial setting time (min)	215	-	-
Final setting time (min)	279	-	-
Compressive strength (3 d, MPa)	24.5	-	-
Compressive strength (28 d, MPa)	48.2	-	-
Solid content (%)	-	-	50±1
Fusing point (°C)	-	40–48	-
Dissolubility	-	Soluble in water	-
Appearance	Grey powder	White powder	White lotion
pH	-	11–13	6–7
Viscosity (mPa·s)	-	-	1000–1200

Note: "–" indicates not measured or not applicable.

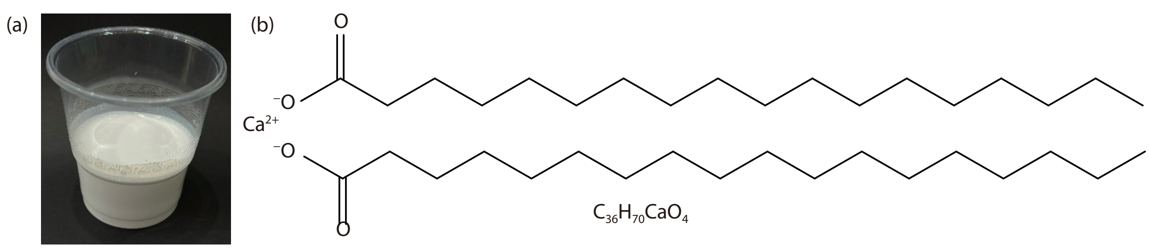

Fig. 5. (a) Apparent morphology and (b) molecular structure of CSE.

Table 3. Physical properties of CSE.

Parameters	Solid content (%)	pH	Viscosity (mPa·s)	Density (g cm^{-3})
Values	42±2	9–12	≤500	1.0–1.1

gates with PG or CPG. Before substitution, the graded aggregates conformed to the skeleton-void structure composed of RCA, NA, and fillers, denoted as the RCA gradation. After substitution, they were changed to the skeleton-suspension structure composed of RCA, CPG (or PG), NA, and fillers, denoted as CPG (or PG)/RCA gradation. Table 4 and Fig. 6 provide the aggregate gradations and the corresponding gradation curves of the base course mixtures, respectively.

(2) Optimum moisture content and maximum dry density

According to ASTM D698, the compaction test for cementitious stabilized materials was conducted to determine the moisture content–dry density relationship curve of the base course mixture. Based on this relationship, the optimum moisture content (OMC) and maximum dry density (MDD) were determined for preparing different test specimens. The results of the compaction test are shown in Fig. 7 and Table 5.

(3) Mix proportions of all designed base course mixtures

To evaluate the performance enhancement of various additives, the mix proportions for the CPG/RCA base course mixtures were determined through a comparative design, as detailed in Table 6. The dosage for each additive was based on the optimal values established in our previous study[29], which systematically analyzed the effects of additives on the mechanical properties and microstructure of the base course, while the current study focuses on evaluating the performance of modified CPG/RCA materials from the perspective of durability.

3.2.2. Specimen preparation for tests

The WDCT, FTCT, DST, and FT are normally adopted to characterize the durability and other properties of materials under

Table 4. Aggregate gradations of base course mixtures.

Mesh size (mm)	Passing percentage (%)				
	Upper limit	Lower limit	RCA gradation	PG/RCA gradation	CPG/RCA gradation
0.075	5	2	3	2.4	2.4
0.15	7	3	5	4.6	4.6
0.3	10	5	7	12.5	12.5
0.6	15	8	11	29.7	29.7
1.18	22	13	17	34.5	34.5
2.36	31	22	26	41.6	41.6
4.75	45	35	40	52.6	52.6
9.5	72	59	65	72.4	72.4
13.2	86	76	81	85	85
16	93	88	90	92.1	92.1
19	100	100	100	100	100

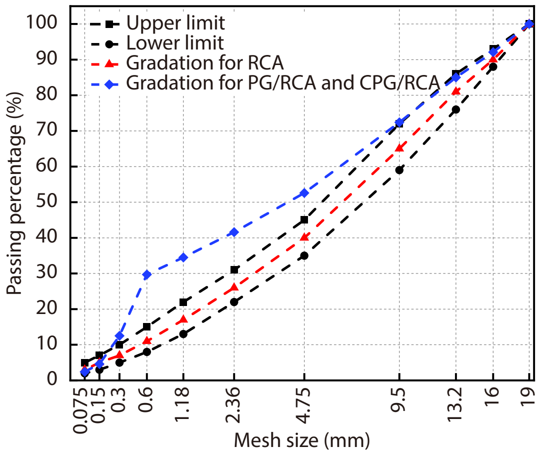

Fig. 6. The gradation curves of base course mixtures.

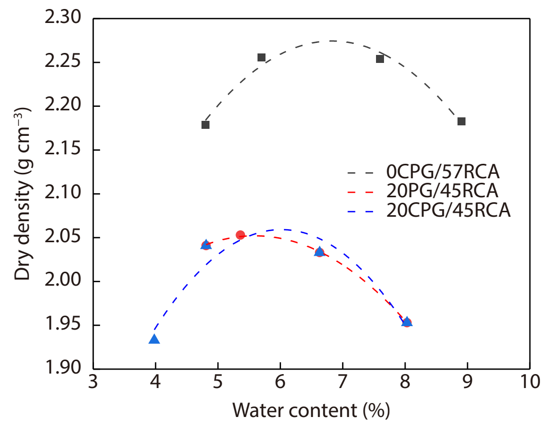

Fig. 7. Relationship between water content and dry density of base course materials.

specific conditions. In this study, they were used to evaluate whether the road base mixture can meet the requirements for pavement usage. Prior to the tests, the corresponding specimens were fabricated and cured according to ASTM D559, ASTM C666, ASTM C157, and ASTM D8044. The fabrication method of the specimens is shown in Fig. 8, while the shape and dimensions of the specimens for different tests are presented in Table 7.

3.3. Testing method

3.3.1. Dry-wet cycle test

The dry-wet cycle test (WDCT) was conducted in this study to evaluate the moisture-induced damage of the prepared base course mixtures according to ASTM D559. Under standard conditions, the prepared CPG/RCA base course mixtures were cured for 6 d. After curing, the samples were dried in an oven

Table 5. The determined OMC and MDD values of base course materials.

Item	Cement (%)	CPG (%)	PG (%)	NA (%)	RCA (%)	OMC (%)	MDD (g cm^{-3})
0CPG/57RCA	5	0	0	38	57	6.73	2.272
20PG/45RCA	5	0	20	30	45	5.97	2.059
20CPG/45RCA	5	20	0	30	45	6.17	2.044

Table 6. Mix design of target base course mixtures.

Abbreviation	CSE (%)	SMN (%)	ESBR (%)	Cement (%)	PG (%)	CPG (%)	RCA (%)	NA (%)
RCA	0	0	0	5	0	0	57	38
PG/RCA	0	0	0	5	20	0	45	30
CPG/RCA	0	0	0	5	0	20	45	30
CPG/RCA-S	0	2.2	0	5	0	20	45	30
CPG/RCA-SC	0.32	2.2	0	5	0	20	45	30
CPG/RCA-SCE	0.32	2.2	1	5	0	20	45	30

Note: S denotes SMN, SC denotes the combined addition of SMN and CSE, and SCE denotes the combined addition of SMN, CSE, and ESBR.

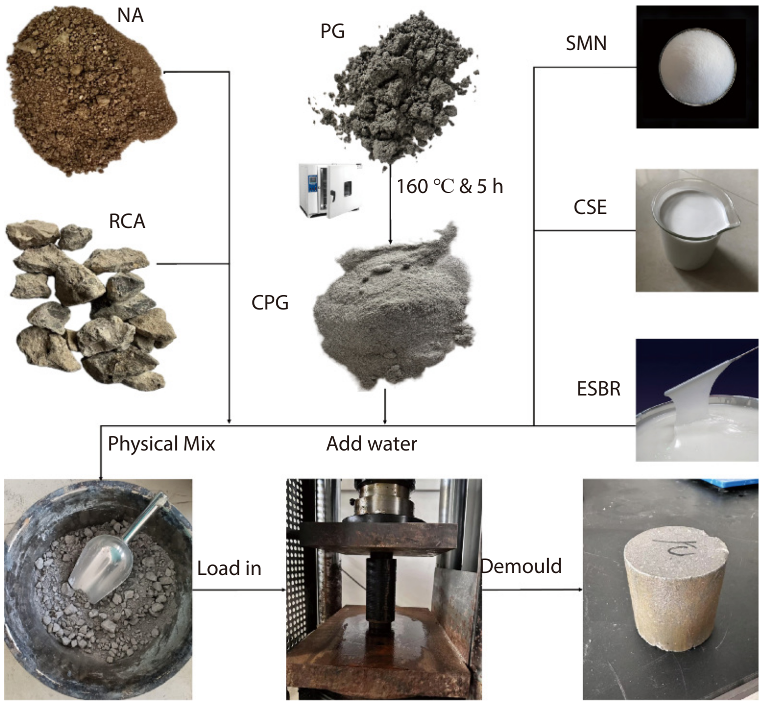

Fig. 8. The fabrication method of the specimens.

Table 7. Fabrication and testing programs for different studied mixtures.

Property	Fabrication method	Sample dimension	Test	Test standard
Dry-wet resistance	Cyclic soak and pressurization	Φ100 mm × 100 mm	WDCT	ASTM D559
Freeze-thaw resistance	Cyclic soak and pressurization	Φ100 mm × 100 mm	FTCT	ASTM C666
Dry shrinkage property	Cyclic soak and pressurization	100 mm × 100 mm × 400 mm	DST	ASTM C157
Fatigue performance	Semi-circular bending	Φ100 mm × 100 mm	FT	ASTM D8044

at 40 °C for 1 d and then soaked in 20 °C water for 1 d, which constituted a dry-wet cycle. To assess the resistance of the prepared base course mixtures to water damage, the tests on unconfined compressive strength and mass loss were performed after five dry-wet cycles. Equation (1) is used to calculate the strength variation.

$$W_n = \frac{m_n - m_{n-1}}{m_{n-1}} \times 100\% \tag{1}$$

where, W_n refers to the strength variation of the sample after n dry-wet cycles (%), and m_n refers to the compressive strength of the sample after n dry-wet cycles (MPa).

3.3.2. Freeze-thaw cycle test

As per ASTM C666, the prepared CPG/RCA and other control samples were first subjected to a 28-day curing period under typical conditions, and then these cured samples were taken out and placed in a −18 °C cold chamber for 16 h for freezing. Following the freezing test, some samples were removed for weighing and then placed into a 20 °C water tank for thawing over the course of 8 h. This process is known as a freeze-thaw cycle. In this study, five freeze-thaw cycles were designed to evaluate the resistance of the prepared base course mixtures to freeze-thaw damage. Equation (2) is used to calculate the frost resistance index:

$$RCSR = \frac{m_n}{m_c} \times 100\% \tag{2}$$

where, $RCSR$ refers to the residual compressive strength rate of the sample (%), m_n refers to the compressive strength of the sample after n freeze-thaw cycles (MPa), and m_c refers to the compressive strength of the control sample (MPa).

3.3.3. Dry shrinkage test

As per ASTM C157, the prepared 100 mm × 100 mm × 400 mm center-beam sample was placed on the laboratory's homemade shrinkage equipment with the dial gauges fixed on the two ends. The displacement sensor of the dial gauge indicates a change when the sample experiences volumetric shrinkage as a result of water loss, making it possible to determine the shrinkage deformation value of the sample by monitoring the dial gauge readings.

3.3.4. Fatigue test

The fatigue test method used in this study was the semi-circular bending (SCB) test[32]. In order to assess the effect of CSE and SMN additives on the fatigue performance of CPG/RCA base course samples, the SCB test was performed in a stress-controlled mode using the UTM testing equipment. A half-sine loading form was applied with a loading frequency of 2 Hz. The test was carried out at 25 °C.

The maximum load of each group of specimens was determined by the SCB test in accordance with the aforementioned fatigue test procedure, and the fracture strength K_{IC} of the specimens was calculated using Equations (3)–(6). Loading levels were set at 40%, 50%, 60%, 70%, and 80% of the fracture strength K_{IC}, and the stress ratio was between 0.4 and 0.8. Fig. 9 shows the fatigue test procedure and the loading method. The fatigue performance of the RCA sample cannot adequately be evaluated by only comparing fatigue life, as each sample has a different fracture strength. Thus, as illustrated in Equations (3) to (6), a power function linear regression curve is fitted to the relationship between fatigue life and stress intensity factor, describing the fatigue performance of the mixes through the functional relationship.

$$\sigma_0 = \frac{P}{2rt} \tag{3}$$

$$Y_{I(0.8)} = 4.782 + 1.219\left(\frac{a}{r}\right) + 0.063exp\left(7.045\left(\frac{a}{r}\right)\right) \tag{4}$$

$$K_{IC} = Y_I\sigma_0\sqrt{\pi a} \tag{5}$$

$$N_f = K \times k_I^{-n} \tag{6}$$

where, K_{IC} refers to fracture toughness (MPa·m$^{0.5}$), P refers to peak load (N), t refers to sample thickness (m), r refers to sample radius (m), Y_I refers to standard stress intensity factor (dimensionless), a refers to the length of the slit (m), and N_f refers to load quantity when sample is broken.

4. Results and discussion

4.1. Dry-wet resistance

Prior to the dry-wet resistance evaluation, the effects of treatment methods on the 7-day unconfined compressive strength of CPG/RCA base course material are analyzed for comparisons, as displayed in Fig. 10. It is observed that compared to the RCA-type (4.79 MPa), PG/RCA and CPG/RCA types reach 3.34 MPa and 4.08 MPa in 7-day unconfined compressive strength, decreased by 30.14% and 14.83%, respectively. These results indicate that the addition of PG and CPG reduces the early strength of the materials. The reason for this phenomenon is that PG reacts with cement during the hydration process to form expansive ettringite (AFt), which may induce microcracks within the matrix, thereby compromising the compressive strength. In contrast, the incorporation of SMN, CSE, and ESBR enhances the material strength. This improvement can be attributed to the fact that SMN, CSE, and ESBR effectively activate the cement hydration process, promoting the formation of denser hydration products and optimizing the microstructure of the composite material. The divergent effects of additives highlight the critical role of chemical compatibility in designing cement-stabilized recycled aggregates for strength development.

Fig. 11 reflects the effect of dry-wet cycles on the unconfined compressive strength of CPG/RCA base course materials after 7-day curing. In contrast to the results shown in Fig. 10, after one dry-wet cycle, the compressive strength of RCA, PG/RCA, CPG/RCA, CPG/RCA-S, CPG/RCA-SC, and CPG/RCA-SCE types increases from 4.79, 3.34, 4.08, 5.37, 5.48, and 5.38 MPa to 5.03, 3.45, 4.32, 5.61, 5.97, and 5.65 MPa, respectively.

Furthermore, the compressive strengths start decreasing from the third dry-wet cycle, and remain 3.15, 3.92, 4.6, 5.36, 5.66, and 5.39 MPa at the fifth cycle for RCA, PG/RCA, CPG/RCA, CPG/RCA-S, CPG/RCA-SC, and CPG/RCA-SCE types, respectively. It is worthwhile noting that although CPG/RCA-

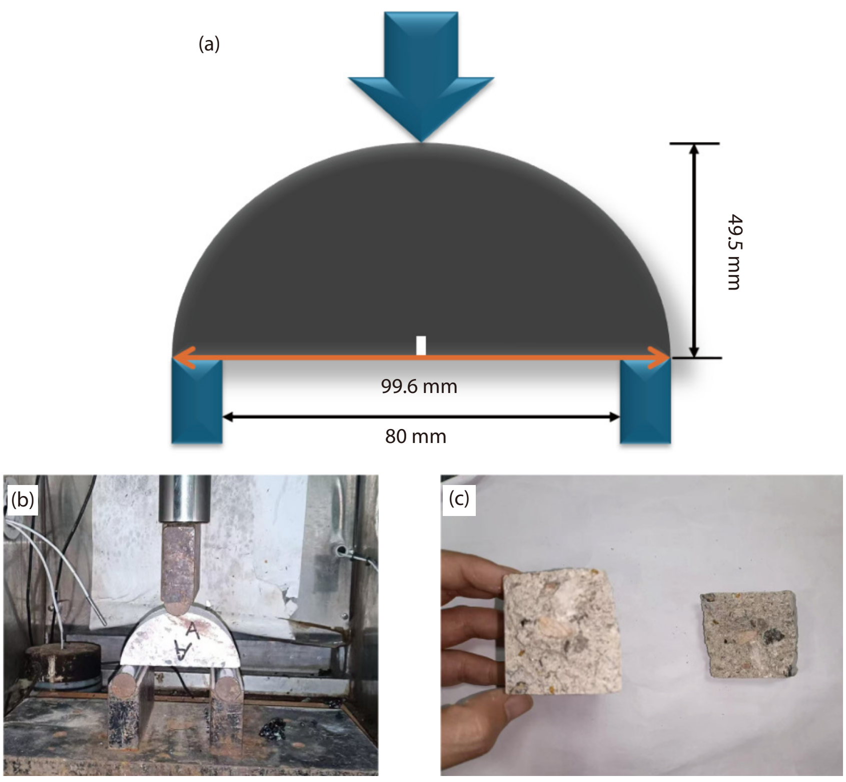

Fig. 9. Loading method and process of fatigue test: (a) sample size, (b) sample loading, (c) sample destruction.

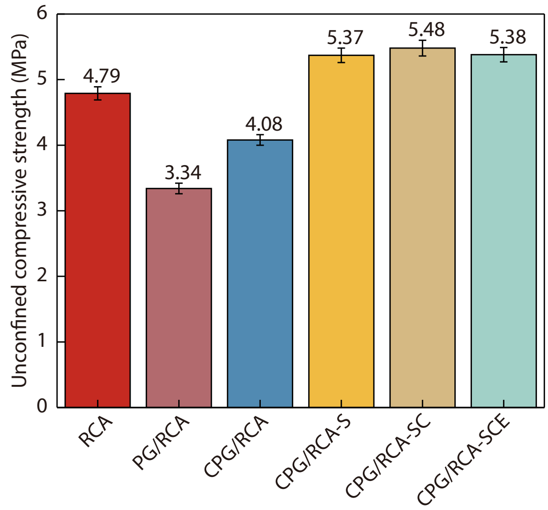

Fig. 10. Effects of treatment methods on the 7-day unconfined compressive strength of CPG/RCA base course material.

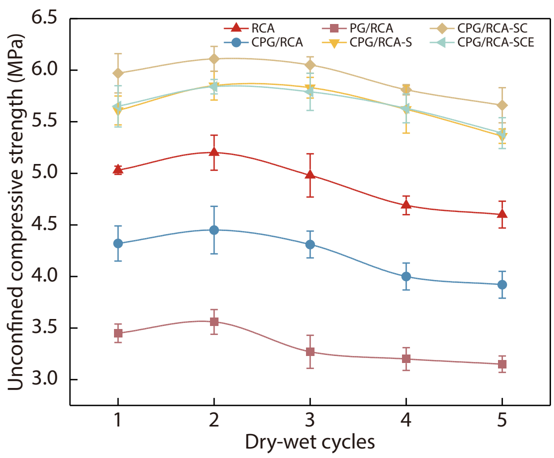

Fig. 11. Effect of dry-wet cycle on the unconfined compressive strength of CPG/RCA base course materials after 7-day curing.

SCE type decreases in compressive strength to some extent within five cycles compared to CPG/RCA-SC type, it still has similar results to that of CPG/RCA-S type. The results indicate that the optimal incorporations of SMN and CSE can not only compensate for the strength loss of 7-day-cured CPG/RCA base course material but also contribute to increasing the strength at the earlier stage of dry-wet cycles, although ESBR will slightly cut down some of the increased strength. This depends on the fact that the mixing of SMN and CSE can produce more chemical opportunities towards hydrations for stabilization and coating of RCA, CPG, and other aggregates in terms of strength enhancement and waterproofing improvement, while the organic coatings of ESBR work to mainly enhance the flexibility and resilience, which results in reduced strength[33,34].

Fig. 12 illustrates the strength variation of 7-day-cured CPG/RCA base course materials with dry-wet cycles. As clearly observed, the strength variation trends differed among the mixtures. After the third cycle, all mixtures exhibited a decrease in unconfined compressive strength. Mixtures like CPG/RCA-SCE and CPG/RCA-SC maintained higher strength

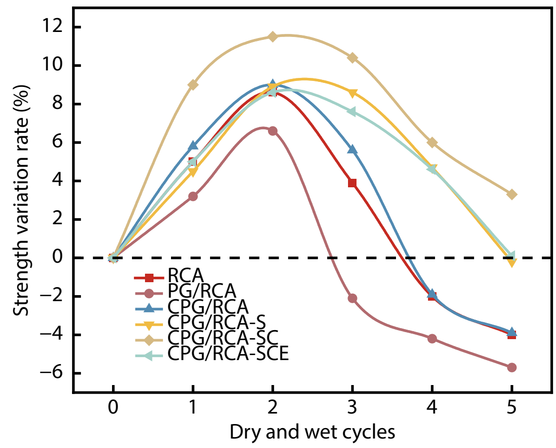

Fig. 12. Strength variation of 7-day-cured CPG/RCA base course materials with dry-wet cycles.

compared to others after several cycles, while mixtures like PG/RCA and CPG/RCA showed a more gradual and consistent decrease in strength. The results suggest that the rate of strength loss is significantly influenced by the material composition and the ability of the mixtures to retain water. Some mixtures exhibited slower strength loss and better resistance to moisture fluctuations, while others showed more rapid deterioration. The reason for the results is that the high-water retention capacity of CPG/RCA-SC contributed to better moisture resistance during the dry-wet cycles, which helped minimize strength loss.

4.2. Freeze-thaw resistance

To better understand the freeze-thaw resistance of CPG/RCA base course materials, the effects of the treatment methods on their 28-day unconfined compressive strengths are shown in Fig. 13. Significantly, compared to the RCA type, the PG/RCA type shows a lower compressive strength of 4.03 MPa, decreased by 2.20 MPa. When CPG is used to replace PG, the compressive strength of the CPG/RCA type comes back to 4.92 MPa, which still doesn't catch up with 6.23 MPa of the RCA type. As the additives are further added into the

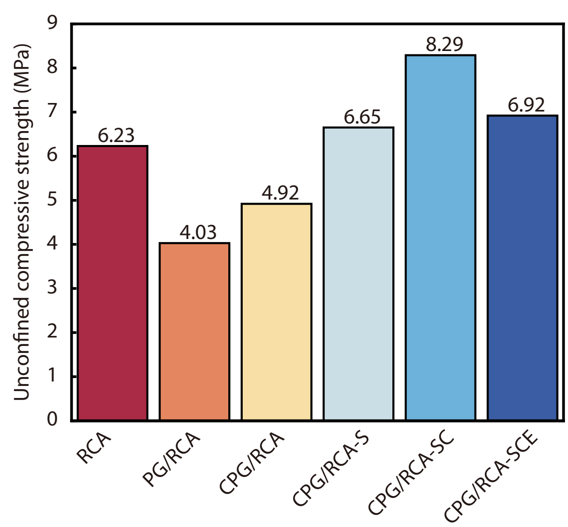

Fig. 13. Effects of treatment methods on the 28-day unconfined compressive strength of CPG/RCA base course material.

CPG/RCA type, the compressive strengths of CPG/RCA-S, CPG/RCA-SC, and CPG/RCA-SCE types are increased to 6.65, 8.29, and 6.92 MPa, respectively, which are all higher than that of the RCA type. It is noteworthy that with the incorporation of ESBR, the compressive strength of the CPG/RCA-SCE type doesn't show a desired increase but rather a slight decrease. The results suggest that the collective use of SMN and CSE can significantly enhance the long-term strength of CPG/RCA base course material, whereas ESBR exerts a certain degree of negative impact on the strength. This is because SMN and CSE partake in the hydration reaction of the CPG/RCA base material mixture, generating inorganic cementitious substances that contribute to the enhancement of strength[35,36]. Conversely, ESBR forms an organic layer at the internal interfaces, which serves to augment the flexibility of the mixture, albeit at the expense of a certain reduction in compressive capacity.

Fig. 14 shows the effect of freeze-thaw cycles on the unconfined compressive strength of CPG/RCA base course materials after 28-day curing. It is clear that, with the increase in freeze-thaw cycles, the compressive strength of all base course materials exhibits a uniform downward trend. During the whole freeze-thaw process, the strength ranking among the types is CPG/RCA-SC > CPG/RCA-SCE > CPG/RCA-S > RCA > CPG/RCA > PG/RCA, with respective values of 5.96, 4.93, 4.41, 4.12, 2.49, and 1.48 MPa after the fifth cycle. Among them, except for PG/RCA and CPG/RCA types, other types have residual strength far exceeding 3 MPa as required for the least applicability. The results indicate that the degradation effect of freeze-thaw cycles on the compressive strength of various base course materials is notably significant, whereas the synergistic use of SMN, CSE, and ESBR can enable the CPG/RCA base course material to endure a greater number of freeze-thaw cycles for practical application.

Fig. 15 exhibits the residual compressive strength ratio of 28-day-cured CPG/RCA base course materials with freeze-thaw cycles. It is obvious that the residual strength ratio of all materials presents a uniform decreasing trend to different extents, where the PG/RCA and CPG/RCA types have similar residual compressive strength ratios at the first four cycles

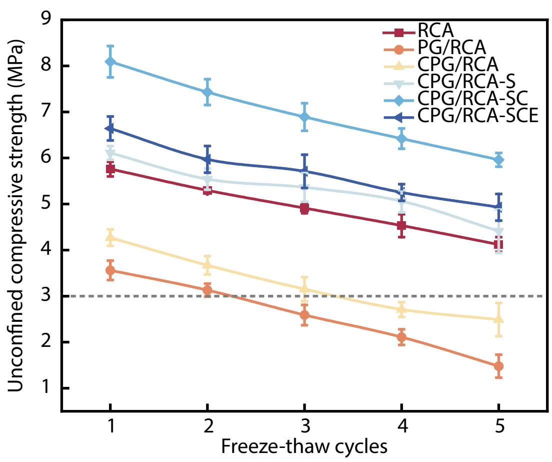

Fig. 14. Effect of freeze-thaw cycle on the unconfined compressive strength of CPG/RCA base course materials after 28-day curing.

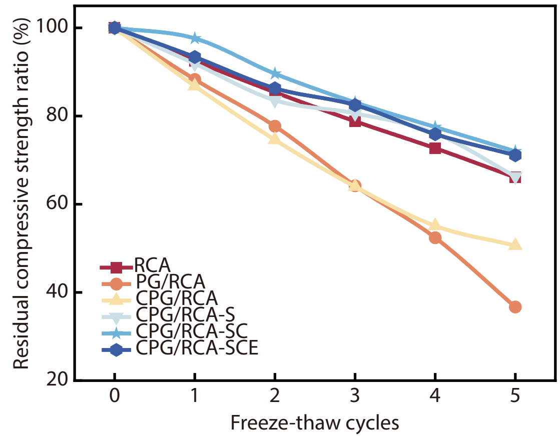

Fig. 15. Residual compressive strength ratio of 28-day-cured CPG/RCA base course materials with freeze-thaw cycles.

and then remain levels of 36.7% and 50.6%, respectively, at the fifth cycle. It is worthwhile noting that the residual compressive strength ratio of the RCA type is much higher than that of these two types, which can still reach 66.1% at the fifth cycle. The results suggest that the utilization of calcination methods to treat PG evidently does not resolve the issue of freeze-thaw resistance in CPG/RCA base course materials, and even so, it still falls short of the freeze-thaw resistance level exhibited by the RCA base course material. Based on this, as the additives are added, the CPG/RCA-S, CPG/RCA-SC, and CPG/RCA-SCE types show improved residual compressive strength ratios, reaching at 66.3%, 72%, and 71.1% while being subjected to five cycles. This result indicates that the incorporation of SMN, CSE, and ESBR has markedly enhanced the residual compressive strength ratio of CPG/RCA base course materials under multiple freeze-thaw cycles, thereby endowing them with the potential for long-term application in cold climatic conditions.

4.3. Dry shrinkage property

Fig. 16 reflects the effect of treatment methods on the dry shrinkage strain development of CPG/RCA base course material within 180 d. It is clear that a significant change in dry shrinkage strain occurs during the first 30 d for all materials, and after that, the rate of dry shrinkage slows down with a small change from 30 d to 180 d. Meanwhile, the changing extent of the dry shrinkage strain follows the order: RCA > PG/RCA ≈ CPG/RCA > CPG/RCA-S > CPG/RCA-SC > CPG/RCA-SCE in type, within 180 d, and at the final day, the dry shrinkage strain of the CPG/RCA-SCE type (namely 570×10^{-6}) is much lower than that of others, particularly the RCA type (1172.5×10^{-6}). The results show that PG and CPG possess a similar capacity to reduce the dry shrinkage strain of RCA base course material and improve dimensional stability, while the sequential addition of SMN, CSE, and ESBR further mitigates the risk of cracking in CPG/RCA base course material caused by shrinkage variations. This phenomenon arises because PG and CPG exhibit a certain degree of water-absorbing expansion, partially counteracting the shrinkage induced by the hydration reaction of RCA base course material, while SMN, CSE, and ESBR play roles in water consumption and infiltra-

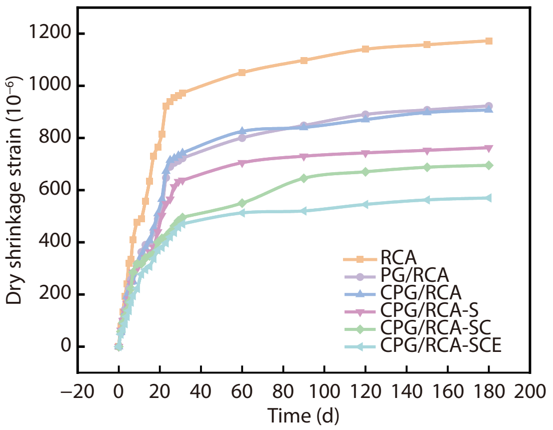

Fig. 16. Effect of treatment methods on the dry shrinkage strain development of CPG/RCA base course material within 180 d.

tion prevention for further reducing the shrinkage of CPG/RCA base material[37].

Fig. 17 illustrates the effect of treatment methods on the total shrinkage of CPG/RCA base course material at 180 d. It can be seen that the RCA type shows the highest total shrinkage at 0.469 mm, and as the PG or CPG is added for graded replacements, the values of PG/RCA and CPG/RCA types are 0.369 mm and 0.363 mm, respectively. Furthermore, with the addition of additives, the values of CPG/RCA-S, CPG/RCA-SC, and CPG/RCA-SCE types are decreased to 0.305 mm, 0.278 mm, and 0.228 mm, respectively. The results also reveal that the combined effects of SMN, CSE, and ESBR can more effectively mitigate the dry shrinkage of CPG/RCA base course material over time.

4.4. Fatigue performance

Fig. 18 displays the fitted fatigue curves showing the effect of treatment methods on fatigue life of CPG/RCA base course materials. Based on this, their corresponding fitted fatigue equations and correlation coefficients are presented in Table 8. From them, it is evident that all the fitted results have the R^2 values greater than 0.9, which are considered reliable for reflecting their fatigue behaviors. From Fig. 18, it is clear that compared to the RCA type, when PG is directly used as a replacement, the PG/RCA type exhibits a significantly diminished fatigue life with the increasing stress intensity factor. However, when CPG is used to substitute for PG, the fatigue life of CPG/RCA type recovers to some extent, approaching that of the RCA type during the stress-loading period. Further, as the SMN is added, the fatigue life of CPG/RCA-S type presents very similar changes to that of RCA type. More notably, the fatigue life of CPG/RCA-SC and CPG/RCA-SCE types is obviously higher than that of CPG/RCA-S type while loaded, particularly the latter.

In addition, as presented in Table 8, it is evident that, as the additives are added, the *k*-value of the CPG/RCA type is increased from 17.131 to 33.819, 81.398, and 418.287 for the CPG/RCA-S, CPG/RCA-SC, and CPG/RCA-SCE types, respectively. Obviously, the addition of SMN increased the *k*-value of CPG/RCA for improved resistance to fatigue; while the incor-

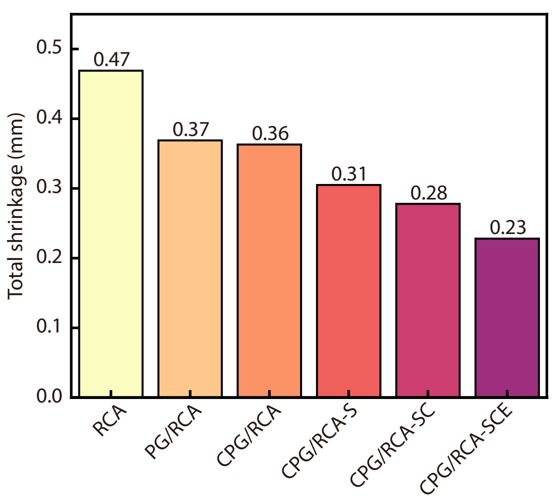

Fig. 17. Effect of treatment methods on total shrinkage of CPG/RCA base course material at 180 d.

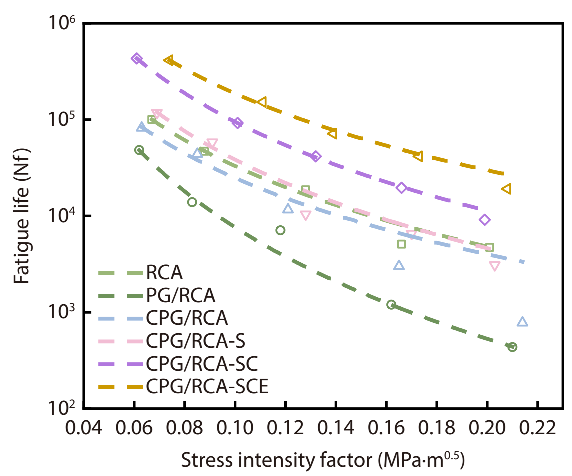

Fig. 18. Fitted fatigue curves showing the effect of treatment methods on fatigue life of CPG/RCA base course materials.

Table 8. Fitted fatigue equations and correlation coefficients of the studied base course materials.

Material type	Fitted fatigue equation	Regression coefficient		R^2
		k	*n*	
RCA	$N_f = 55.125 \times K_I^{-2.778}$	55.125	2.778	0.998
PG/RCA	$N_f = 1.083 \times K_I^{-3.848}$	1.083	3.848	0.992
CPG/RCA	$N_f = 17.131 \times K_I^{-2.632}$	17.131	3.071	0.998
CPG/RCA-S	$N_f = 33.819 \times K_I^{-3.056}$	33.819	3.056	0.981
CPG/RCA-SC	$N_f = 81.398 \times K_I^{-3.067}$	81.398	3.067	0.999
CPG/RCA-SCE	$N_f = 418.287 \times K_I^{-2.649}$	418.287	2.649	0.997

poration of CSE and ESBR orderly produces better effects, further raising the *k*-value and thereby decreasing the cracking risk caused by fatigue behavior. It is noteworthy that a comparative analysis of *n*-value for all types indicates that the CPG/RCA-SCE type has the lowest result of 2.649, showing the smallest susceptibility to repeated loads.

The abovementioned results suggest that the use of CPG cannot fully solve the issue of fatigue life loss caused by the direct use of PG in RCA base course material, but the adoption of ESBR, with a combined use of SMN and CSE, shows a positively surprising improvement in extending the fatigue life of CPG/RCA base course material. The reason is that the organic layers of demulsified ESBR can be formed and existed in the interfacial zones resulting from physicochemical interactions from SMN and SCE among RCA, CPG, and other aggregates, which thus provides the multiple benefits in enhanced stress absorption, improved bonding strength, and reduced void ratio in the CPG/RCA mixture, enabling it to withstand more cycles of loads.

5. Conclusions

This study focused on the sustainable recycling of PG and RCA into the base course for pavement construction, aiming to mitigate moisture-induced damage and improve durability. After converting PG to calcined PG (CPG), the combined use of SMN, CSE, and ESBR, as strength-enhancing, water-preventing, and flexibility-improving additives, was considered to solve the durability issue of CPG/RCA base course materials. Based on the dry-wet cycle test, freeze-thaw cycle test, shrinkage test, and fatigue test, the moisture-induced performance and durability of base course materials were comparatively analyzed. Some concluding findings can be drawn as follows:

(1) WDCT results show that PG and CPG reduced 7-day strength by 30.14% and 14.83%, respectively. SMN and CSE mitigated this loss, with CPG/RCA-SC retaining 5.66 MPa after five cycles. These additives effectively stabilized the matrix structure, although ESBR caused a marginal decrease in the final strength.

(2) FTCT evaluations reveal that CPG/RCA-SC reached a 28-day strength of 8.29 MPa. Its residual strength ratio after five cycles was 72%, significantly exceeding those of PG/RCA (36.7%) and CPG/RCA (50.6%). The synergy of SMN, CSE, and ESBR markedly enhanced long-term durability for cold environment applications.

(3) DST results indicate that CPG/RCA-SCE reduced the 180-day strain from 1172.5×10^{-6} (RCA) to 570×10^{-6}, and decreased the total shrinkage from 0.469 mm (RCA) to 0.228 mm. These results prove that additives inhibit shrinkage-induced cracking and enhance dimensional stability.

(4) FT results show that the *k*-value is markedly increased from 1.083 (PG/RCA type) to 418.287 (CPG/RCA-SCE type), representing a vast enhancement in fatigue resistance.

In summary, the proposed method paves the way for novel approaches in the recycling and application of PG and RCA in forthcoming pavement base constructions. The findings of this study offer valuable insights for the engineering implementation of PG/RCA base course in pavement. Nonetheless, specific durability evaluations, especially concerning the long-term water resistance and climate resilience of the PG/RCA base course, require further extensive examination in laboratory settings. Consequently, subsequent research endeavors should integrate comprehensive laboratory analyses with field durability tests to advance the progression of engineering applications.

Author contribution statement

Jinxiong Huang: Data curation, Formal analysis, Methodology, Writing – original draft, Writing – review & editing. **Xiong Xu:** Conceptualization, Formal analysis, Funding acquisition, Methodology, Resources, Writing – original draft, Writing – review & editing. **Kazi Rajibul Alam:** Data curation, Investigation, Methodology, Software. **Yang Wu:** Data curation, Formal analysis, Methodology, Writing – original draft, Writing – review & editing. **Chiyao Qu:** Formal analysis, Methodology, Writing – original draft, Writing – review & editing. **Jiapei Wang:** Formal analysis, Investigation, Methodology.

Declaration of competing interest

The authors declare that they have no known competing financial interests or personal relationships that could have appeared to influence the work reported in this paper.

Acknowledgments

The authors gratefully acknowledge the Major Program (JD) of Hubei Province (2025BEA005) for providing the research funds.

References

[1] Gu, J., Liu, X., Zhang, Z. Road base materials prepared by multi-industrial solid wastes in China: A review. *Construction and Building Materials*, **2023**, 373: 130860. https://doi.org/10.1016/j.conbuildmat.2023.130860.

[2] Xu, X., Leng, Z., Lan, J., et al. Sustainable practice in pavement engineering through value-added collective recycling of waste plastic and waste tyre rubber. *Engineering*, **2021**, 7(6): 857–867. https://doi.org/10.1016/j.eng.2020.08.020.

[3] Li, S., Yu, J., Wei, R., et al. Innovative reaction-rejuvenation of aged SBS modified asphalt binder: From physico-rheological behavior to rejuvenation mechanism. *Developments in the Built Environment*, **2026**, 25: 100822. https://doi.org/10.1016/j.dibe.2025.100822.

[4] Fang, K., Xu, L., Yang, M., et al. One-step wet-process phosphoric acid by-product $CaSO_4$ and its purification. *Separation and Purification Technology*, **2023**, 309: 123048. https://doi.org/10.1016/j.seppur.2022.123048.

[5] Tayibi, H., Choura, M., López, F. A., et al. Environmental impact and management of phosphogypsum. *Journal of Environmental Management*, **2009**, 90(8): 2377–2386. https://doi.org/10.1016/j.jenvman.2009.03.007.

[6] Attallah, M. F., Metwally, S. S., Moussa, S. I., et al. Environmental impact assessment of phosphate fertilizers and phosphogypsum waste: Elemental and radiological effects. *Microchemical Journal*, **2019**, 146: 789–797. https://doi.org/10.1016/j.microc.2019.02.001.

[7] Chen, X., Gao, J., Zhao, Y. Investigation on the hydration of hemihydrate phosphogypsum after post treatment. *Construction and Building Materials*, **2019**, 229: 116864. https://doi.org/10.1016/j.

conbuildmat.2019.116864.
[8] Chen, X., Wu, Q., Gao, J., et al. Hydration characteristics and mechanism analysis of β-calcium sulfate hemihydrate. *Construction and Building Materials*, **2021**, 296: 123714. https://doi.org/10.1016/j.conbuildmat.2021.123714.
[9] Li, C., Dong, Y., Yi, Y., et al. Effects of phosphogypsum on enzyme activity and microbial community in acid soil. *Scientific Reports*, **2023**, 13: 6189. https://doi.org/10.1038/s41598-023-33191-2.
[10] Huang, X., Xu, X., Xu, G., et al. New insights into value-added application of phosphogypsum in asphalt mixture through chemical stabilization of polymeric methylene diphenyl diisocyanate. *Cleaner Materials*, **2025**, 18: 100349. https://doi.org/10.1016/j.clema.2025.100349.
[11] Amrani, M., Taha, Y., Kchikach, A., et al. Phosphogypsum recycling: New horizons for a more sustainable road material application. *Journal of Building Engineering*, **2020**, 30: 101267. https://doi.org/10.1016/j.jobe.2020.101267.
[12] Liu, Y., Wang, Y., Chen, Q. Using cemented paste backfill to tackle the phosphogypsum stockpile in China: A down-to-earth technology with new vitalities in pollutant retention and CO_2 abatement. *International Journal of Minerals, Metallurgy and Materials*, **2024**, 31(7): 1480–1499. https://doi.org/10.1007/s12613-023-2799-y.
[13] Geraldo, R. H., Costa, A. R. D., Kanai, J., et al. Calcination parameters on phosphogypsum waste recycling. *Construction and Building Materials*, **2020**, 256: 119406. https://doi.org/10.1016/j.conbuildmat.2020.119406.
[14] Liu, G., Guan, B., Liang, Y., et al. Preparation of phosphogypsum (PG) based artificial aggregate and its application in the asphalt mixture. *Construction and Building Materials*, **2022**, 356: 129218. https://doi.org/10.1016/j.conbuildmat.2022.129218.
[15] Liu, S., Ouyang, J., Ren, J. Mechanism of calcination modification of phosphogypsum and its effect on the hydration properties of phosphogypsum-based supersulfated cement. *Construction and Building Materials*, **2020**, 243: 118226. https://doi.org/10.1016/j.conbuildmat.2020.118226.
[16] Deng, F., Ye, J., Liu, Y., et al. Influence of cement on properties of calcined phosphogypsum based composite cementitious materials. *Journal of Materials Research and Technology*, **2023**, 24: 3145–3156. https://doi.org/10.1016/j.jmrt.2023.03.194.
[17] Xu, X., Luo, Y., Sreeram, A., et al. Potential use of recycled concrete aggregate (RCA) for sustainable asphalt pavements of the future: A state-of-the-art review. *Journal of Cleaner Production*, **2022**, 344: 130893. https://doi.org/10.1016/j.jclepro.2022.130893.
[18] Liu, C., Liu, H., Zhu, C., et al. On the mechanism of internal temperature and humidity response of recycled aggregate concrete based on the recycled aggregate porous interface. *Cement and Concrete Composites*, **2019**, 103: 22–35. https://doi.org/10.1016/j.cemconcomp.2019.04.016.
[19] Zheng, L., Wu, H., Zhang, H., et al. Characterizing the generation and flows of construction and demolition waste in China. *Construction and Building Materials*, **2017**, 136: 405–413. https://doi.org/10.1016/j.conbuildmat.2017.01.055.
[20] Xu, X., Sreeram, A., Leng, Z., et al. Challenges and opportunities in the high-quality rejuvenation of unmodified and SBS modified asphalt mixtures: State of the art. *Journal of Cleaner Production*, **2022**, 378: 134634. https://doi.org/10.1016/j.jclepro.2022.134634.
[21] Bru, K., Touzé, S., Bourgeois, F., et al. Assessment of a microwave-assisted recycling process for the recovery of high-quality aggregates from concrete waste. *International Journal of Mineral Processing*, **2014**, 126: 90–98. https://doi.org/10.1016/j.minpro.2013.11.009.
[22] Sun, C., Chen, Q., Xiao, J., et al. Utilization of waste concrete recycling materials in self-compacting concrete. *Resources, Conservation and Recycling*, **2020**, 161: 104930. https://doi.org/10.1016/j.resconrec.2020.104930.
[23] Piccinali, A., Diotti, A., Plizzari, G., et al. Impact of recycled aggregate on the mechanical and environmental properties of concrete: A review. *Materials*, **2022**, 15(5): 1818. https://doi.org/10.3390/ma15051818.
[24] Gao, C., Huang, L., Yan, L., et al. Strength and ductility improvement of recycled aggregate concrete by polyester FRP-PVC tube confinement. *Composites Part B: Engineering*, **2019**, 162: 178–197. https://doi.org/10.1016/j.compositesb.2018.10.102.
[25] Yuan, W., Li, H., Zhang, D., et al. Effects of the physicochemical properties of sodium metasilicate on the hydration kinetics and high-temperature stability of one-part alkali-activated fly ash-slag materials. *Construction and Building Materials*, **2025**, 491: 142730. https://doi.org/10.1016/j.conbuildmat.2025.142730.
[26] He, G., Kong, D., Chen, X., et al. Preparation of C-S-H gels by mechanochemistry and its influences on properties of super-retarded cement-based materials with sucrose. *Cement and Concrete Composites*, **2024**, 153: 105734. https://doi.org/10.1016/j.cemconcomp.2024.105734.
[27] Wu, S., Zhang, C., Zhou, F., et al. The effect of nano-scale calcium stearate emulsion on the integral waterproof performance and chloride resistance of cement mortar. *Construction and Building Materials*, **2022**, 317: 125903. https://doi.org/10.1016/j.conbuildmat.2021.125903.
[28] Yao, X., Xu, H., Xu, T. Mechanical properties and enhancement mechanisms of cold recycled mixture using waterborne epoxy resin/styrene butadiene rubber latex modified emulsified asphalt. *Construction and Building Materials*, **2022**, 352: 129021. https://doi.org/10.1016/j.conbuildmat.2022.129021.
[29] Wu, Y., Bian, X., Liu, J., et al. Performance improvement and microstructure characterization of cement-stabilized roadbase materials containing phosphogypsum/recycled concrete aggregate. *Materials*, **2023**, 16(19): 6607. https://doi.org/10.3390/ma16196607.
[30] Li, X., Zhang, Q. Dehydration behaviour and impurity change of phosphogypsum during calcination. *Construction and Building Materials*, **2021**, 311: 125328. https://doi.org/10.1016/j.conbuildmat.2021.125328.
[31] Lv, Y., Luo, Y., Song, C., et al. Effect of calcium stearate hydrophobic agent on the performance of mortar and reinforcement corrosion in mortar with cracks. *Construction and Building Materials*, **2024**, 450: 138684. https://doi.org/10.1016/j.conbuildmat.2024.138684.
[32] Dong, S., Hao, P., Wang, J., et al. A novel method for testing the fatigue performance of cement stabilized base field coring samples. *Construction and Building Materials*, **2021**, 274: 122065. https://doi.org/10.1016/j.conbuildmat.2020.122065.
[33] Bualuang, T., Jitsangiam, P., Nusit, K., et al. Enhancing lateritic soil for sustainable pavement subbase with polymer-modified cement: A comparative study of styrene butadiene rubber and styrene acrylic latex applications. *Case Studies in Construction Materials*, **2024**, 21: e03760. https://doi.org/10.1016/j.cscm.2024.e03760.
[34] Zhang, Y., Zhang, A., Kang, L., et al. Mechanical properties and thermal stability of kaolinite/emulsion polymerization styrene butadiene rubber composite prepared by latex blending method. *Polymer Science, Series A*, **2020**, 62(4): 407–421. https://doi.org/10.1134/S0965545X20040112.
[35] Zou, M., He, Z., Xia, Y., et al. High-volume phosphogypsum cement stabilized road base: Preparation methods and strength formation mechanism. *Materials*, **2024**, 17(24): 6201. https://doi.org/10.3390/ma17246201.
[36] Huang, Y., Ma, L., Huang, Z., et al. Effect of stearic acid and sodium stearate on hydrophobicity of nano calcium carbonate and mechanism of water vapor adsorption. *Scientific Reports*, **2025**, 15: 364. https://doi.org/10.1038/s41598-024-82802-z.
[37] Sun, J., Valeriy, Z., Huang, Y., et al. Study on the effect of cationic

latex on the properties of cement stabilized iron tailings. *Journal of Building Engineering*, **2024**, 83: 108337. https://doi.org/10.1016/j.jobe.2023.108337.

Jinxiong Huang is a master's candidate at the School of Civil Engineering and Architecture, Wuhan Institute of Technology. His research interests focus on the comprehensive utilization of industrial solid waste, phosphogypsum-based base course materials, and the mechanical and durability performance of road engineering materials.

Xiong Xu, PhD, was a Postdoctoral Researcher at The Hong Kong Polytechnic University (2018-2020), and is currently an Associate Professor at the School of Civil Engineering and Architecture, Wuhan Institute of Technology, a Master's Supervisor, and an expert reviewer for Hubei Communications Investment Group Smart Traffic Research Institute and the Ministry of Education thesis review. His main research areas include the comprehensive utilization of solid waste, phosphogypsum road engineering technology, rubber asphalt pavement materials, asphalt pavement construction and maintenance technologies, and asphalt pavement recycling technologies. He has led more than 10 projects, including the National Natural Science Foundation of China, Hubei Provincial Natural Science Foundation, Hubei Provincial Department of Education research projects, Hubei Provincial Construction Science and Technology projects, and enterprise-commissioned horizontal projects. He has also been a core participant in international cooperation projects funded by the Hubei Provincial Science and Technology Department, and key R&D projects supported by the same department. He has published over 60 academic papers, including 12 SCI papers in Q1 of the CAS Journal Ranking, one hot/highly cited paper, and one paper selected into the Major Scientific and Technological Innovation Achievements Database in Transport (paper). He has applied for more than 10 patents, with 4 granted. He is an invited reviewer for over 40 academic journals, including *Journal of Cleaner Production*, *Construction and Building Materials*, and *Journal of Materials in Civil Engineering*, and has received several excellent reviewer awards. He serves as a youth editorial board member for the journal *Municipal Engineering Technology* (in Chinese).